

## Scattering of Phonons by Charge Carriers in Superfluid Helium: The Zero-Velocity Limit

K. W. Schwarz

*Department of Physics and The James Franck Institute, The University of Chicago, Chicago, Illinois 60637*  
(Received 14 March 1972)

The problem of phonon scattering by charge carriers in superfluid helium is considered, with the aim of interpreting recent measurements of charge-carrier mobilities below 1 °K. The calculations are done in the hydrodynamic approximation, and explicitly include the effect of the electrostrictive variations in the fluid surrounding the core structures of the carriers. For the positive carrier, the necessary core properties are calculated, and in particular it is found that the core does not act like a hard sphere. The theoretically predicted phonon-limited mobility for positives is found to be in excellent agreement with experiment, provided a liquid-solid surface energy of order 0.1 erg cm<sup>-2</sup> for the core is assumed. In the case of the negatives, results are similar to those of previous workers. The mobility of the electron bubble is substantially explained by resonance scattering of phonons, but a significant discrepancy remains which probably arises from the use of the idealized bubble model. The changes in the theoretical mobility curves that can be produced by varying the bubble parameters  $a_+$  and  $V_1$  are of the order of this systematic discrepancy, so that the best values of these parameters cannot be determined from the data. Values of  $a_+$  less than 15 Å can, however, be ruled out with some confidence. The roton contribution to the scattering is determined by subtracting the phonon part, and turns out to have some unexpected features. For the positives,  $e/\mu_+$   $\cong 1.34 \times 10^{-9} T^{-1/2} e^{-\Delta/kT}$ . The temperature dependence of  $e/\mu_+$  is not as clearly established, but the prefactor lies between  $T^0$  and  $T^{-1/2}$ . The ratio of  $e/\mu_+$  to  $e/\mu_-$  is found to have a surprisingly small value of about 1.5, perhaps indicating that electrostrictive variations in the fluid surrounding the positive core scatter rotons strongly. No present theory of roton scattering explains the observed features.

### I. INTRODUCTION

It has long been realized<sup>1</sup> that at temperatures below  $\sim 0.6$  °K the movement of charge carriers through superfluid helium is limited mainly by their interaction with thermally excited phonons. Recently, detailed experimental studies of the equilibrium drift velocities attained by charge carriers under the influence of a weak electric field have been carried out in this temperature region.<sup>2-4</sup> To interpret such observations one must know how phonons are scattered by the structures associated with the charge carriers in the liquid. Several features of this problem serve to make a simple yet adequate treatment possible. At the low temperatures under consideration, those phonons important to the transport properties of the carriers have wavelengths of several interatomic spacings. They can therefore be described to a reasonable approximation in terms of continuum sound waves. Second, the excess charges are known to be associated with microscopically large structures in the liquid. The negative carrier<sup>5</sup> consists of a deformable electron bubble with a radius of about 15 Å, whereas the positive carrier<sup>6</sup> apparently features a solid central core with a radius of about 6 Å plus appreciable local density and pressure gradients in the surrounding liquid. These accepted theoretical models for the carrier structures are continuum models which average over any detailed ef-

fects arising from the microscopic discreteness of the liquid. Again this cannot be such a bad approximation because of the large sizes of the structures involved, and in fact good agreement with experiment is usually found.

If a continuum picture can reasonably be applied to both the phonons and the charge carriers, then it is proper to treat their interaction as a problem in fluid dynamics. Not only is such an approach entirely self-consistent as regards the kind of approximations made throughout, but it has the necessary virtue of being simple enough to permit detailed computations and comparison with experiment. It has already been successfully applied by Baym *et al.*<sup>7</sup> to explain the motion of the electron bubble in the phonon-limited regime, and the work described below is mainly an attempt to achieve a similar success for the positive carrier. The new elements in our treatment include a somewhat more coherent approach to the hydrodynamic problem, an approach which can readily be generalized to include other cases of physical interest. The effect of the electrostrictive density variations in the fluid on the phonon scattering is explicitly considered and shown to be of major importance for the positive carrier. Detailed comparisons with experiment are made, and good agreement is obtained in the phonon-limited region. The scattering due to rotons is then derived by subtracting the phonon contribution from the experimental data.

## II. BASIC EQUATIONS

The equations of motion of an ideal fluid at  $T=0$  are

$$\rho \left( \frac{\partial \vec{v}}{\partial t} + (\vec{v} \cdot \nabla) \vec{v} \right) = -\nabla p + (\vec{P} \cdot \nabla) \vec{E}, \quad (1)$$

$$\frac{\partial \rho}{\partial t} + \nabla \cdot (\rho \vec{v}) = 0, \quad (2)$$

where Eq. (1) includes the local electrostrictive body force arising from the presence of an excess charge. Here  $\rho$  is the density,  $\vec{v}$  is the fluid velocity,  $p$  is the pressure,  $\vec{P}$  is the polarization per unit volume, and  $\vec{E}$  is the electric field. We assume that to a sufficient approximation one can write  $\vec{P} = \rho N \alpha_0 M^{-1} \vec{E} = \beta \rho \vec{E}$  where  $N$  is Avogadro's number,  $\alpha_0$  is the atomic polarizability, and  $M$  is the molecular weight, so that  $\beta$  equals the polarizability per unit mass. Then Eq. (1) takes the simpler form

$$\frac{\partial \vec{v}}{\partial t} + (\vec{v} \cdot \nabla) \vec{v} = -\frac{\nabla p}{\rho} + \frac{\beta}{2} \nabla \left[ \frac{D^2}{(1 + 4\pi\beta\rho)^2} \right], \quad (3)$$

where  $D$  is the electric displacement field which depends on the instantaneous position  $\vec{r}_0(t)$  of the charge according to

$$\vec{D} = e [ \vec{r} - \vec{r}_0(t) ] / | \vec{r} - \vec{r}_0(t) |^3. \quad (4)$$

To complete the required set of equations we note that below  $1^\circ\text{K}$  the equation of state of the liquid is<sup>8</sup>

$$p = A_1(\rho - \rho_0) + A_2(\rho - \rho_0)^2 + A_3(\rho - \rho_0)^3, \quad (5)$$

where  $\rho_0 = 0.14513$ ,  $A_1 = 5.68 \times 10^8$ ,  $A_2 = 1.110 \times 10^{10}$ ,  $A_3 = 7.41 \times 10^{10}$ , all in cgs units.

There are several distinct problems associated with this set of equations, each having its own particular physical interest. Most simply there is the case of the stationary charge carrier when no sound waves are present. The resulting equations determine the equilibrium density and pressure distributions in the liquid, as has been discussed by Atkins.<sup>6</sup> One may also investigate the more complicated case where the charge carrier is essentially stationary but a sound field is present. This is, of course, the phonon-scattering problem in the continuum approximation and is of considerable interest because, as Baym *et al.*<sup>7</sup> have shown, the calculated scattering cross sections can be directly related to the zero-field mobilities of the carriers. A third problem is the calculation of the velocity field of a moving carrier, which relates particularly to the interpretation of experiments that measure the effective mass of the charge carriers.<sup>9</sup> Finally there is the question of how a moving carrier, with its associated velocity field, scatters sound waves. An understanding of these processes is essential for the intelligent dis-

cussion of such problems as the nonlinear variation of the average drift velocity of the carriers with the electric field. Here we shall limit ourselves to the relatively simple situations where the carriers are stationary. The more complex behavior arising from the motion of the carriers will be considered in a later paper.

## III. ELECTROSTRICTIVE EQUILIBRIUM

A very complete discussion of this aspect has been given by Atkins,<sup>6</sup> and our main purpose here is to briefly review his work and to establish some results which will later prove useful. When all velocities are set equal to zero, Eqs. (2) and (3) reduce to the condition for mechanical equilibrium:

$$\frac{\nabla p}{\rho} = \nabla \left[ \frac{\frac{1}{2} \beta D^2}{(1 + 4\pi\beta\rho)^2} \right]. \quad (6)$$

Using Eqs. (4) and (5), this can then be integrated to yield

$$\begin{aligned} B_1 \ln \left( \frac{\rho_2}{\rho_1} \right) + B_2 (\rho_2 - \rho_1) + B_3 (\rho_2^2 - \rho_1^2) \\ = \frac{\frac{1}{2} \beta e^2}{r_2^4 (1 + 4\pi\beta\rho_2)^2} - \frac{\frac{1}{2} \beta e^2}{r_1^4 (1 + 4\pi\beta\rho_1)^2}, \end{aligned} \quad (7)$$

where  $B_1 = A_1 - 2\rho_0 A_2 + 3\rho_0^2 A_3$ ,  $B_2 = 2A_2 - 6\rho_0 A_3$ , and  $B_3 = \frac{3}{2} A_3$ . Given the density  $\rho_1$  at  $r_1$ , Eq. (7) determines the density  $\rho_2$  at any other radius  $r_2$ . The corresponding pressures are of course derived from Eq. (5). In Figs. 1 and 2 we show the calculated variation with distance from the excess charge of the density and pressure in the surrounding liquid, for various limiting values of the pressure (and hence the density) at infinity. Figures 1 and 2 apply to both negative and positive charges provided we limit their application to radii greater than those of the appropriate core structure. The nature of the core structures will be reviewed later as the need arises.

## IV. SOUND SCATTERING

We denote the electrostrictive equilibrium solutions by a zero subscript, and find the form of the equations governing the sound fields. The similar problem of sound propagating through a nonuniform atmosphere in mechanical equilibrium under a gravitational field is discussed by Lamb.<sup>10</sup> Writing  $\vec{v} = \vec{v}_s$ ,  $p = p_0 + p_s$ ,  $\rho = \rho_0 + \rho_s$  in Eqs. (2) and (3) and linearizing, one obtains

$$\frac{\partial \vec{v}_s}{\partial t} = -\nabla \left( \frac{\rho_s}{\rho_0} \right) \quad (8)$$

and

$$\frac{1}{c_0^2} \frac{\partial p_s}{\partial t} + \nabla \cdot (\rho_0 \vec{v}_s) = 0, \quad (9)$$

where we have used  $\rho_s = (\partial\rho/\partial p)_0 p_s = p_s/c_0^2$  to eliminate  $\rho_s$ . In deriving Eqs. (8) and (9), some small

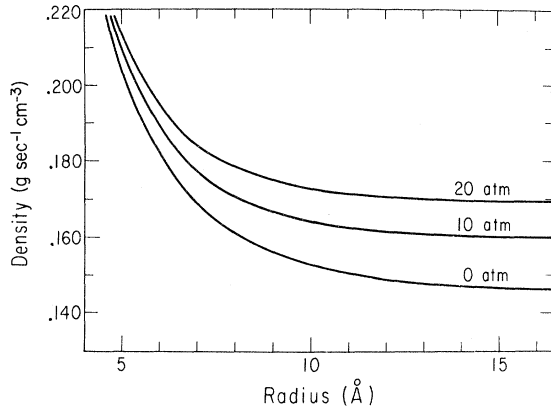


FIG. 1. Electrostrictive variation of fluid density with distance from an excess charge in liquid helium below 1.0 °K, for various values of the pressure at infinity.

terms which arise from the dependence of the local dielectric constant on  $\rho_s$  have been neglected. The neglected terms are typically on the order of a few percent of the retained terms, and thus do not constitute an important source of error. Introducing the velocity potential  $\phi$  defined by  $\vec{v} = \nabla\phi$ , one then obtains

$$\dot{p}_s = -\rho_0 \frac{\partial \phi}{\partial t} \quad (10)$$

and

$$\nabla^2 \phi + \nabla(\ln \rho_0) \cdot \nabla \phi - \frac{1}{c_0^2} \frac{\partial^2 \phi}{\partial t^2} = 0. \quad (11)$$

In interpreting these equations the reader should remember that not only  $\rho_0$ , but the local sound velocity  $c_0$  as well, is a strong function of the radial distance from the excess charge. As seen in Figs. 1 and 2, however, significant variations in these quantities are confined to the immediate vicinity of the charge. At large distances, Eqs. (11) and (12) become the usual equations for sound propagation in a uniform medium.

The scattering problem represented by Eqs. (11) and (12) can be dealt with by straightforward partial-wave analysis. We write

$$\phi = \sum_{l=0}^{\infty} A_l \frac{u_l(r)}{kr} P_l(\cos\theta) e^{-i\omega t} \quad (12)$$

and the associated radial equation is then

$$\frac{d^2 u_l}{dr^2} + \frac{d(\ln \rho_0)}{dr} \frac{du_l}{dr} + \left[ \frac{k^2 c_\infty^2}{c_0^2} - \frac{1}{r} \frac{d(\ln \rho_0)}{dr} - \frac{l(l+1)}{r^2} \right] u_l = 0. \quad (13)$$

Here  $c_\infty$  is the velocity of sound in the bulk liquid and  $k$  is  $\omega/c_\infty$ . The boundary conditions at the radius  $a$  of the core structure are treated in the

manner of Celli *et al.*<sup>11</sup> That is, the response of the core surface

$$a(\theta) = a_0 + \sum_{l=0}^{\infty} \delta a_l P_l(\cos\theta) \quad (14)$$

to the acting excess-pressure field  $\delta p(\theta) = \sum \delta p_l P_l(\cos\theta)$  arising from the sound wave is characterized by the response coefficients  $\lambda_l$ :

$$\delta a_l = \lambda_l \delta p_l. \quad (15)$$

From Eq. (10) one then obtains the boundary condition

$$\frac{d}{dr} \left( \frac{u_l}{r} \right) = \lambda_l \rho_0(a) c_\infty^2 k^2 \left( \frac{u_l}{r} \right) \quad (16)$$

at  $r = a$ .

Equation (13) can be converted into a differential equation for the partial-wave phase shift  $\eta_l$ , using the method due to Levy and Keller<sup>12</sup>:

$$\begin{aligned} \frac{d\eta_l}{dr} = k^2 r^2 \frac{d(\ln \rho_0)}{dr} [j'_l(kr) \cos \eta_l - \eta'_l(kr) \sin \eta_l] \\ \times [j_l(kr) \cos \eta_l - n_l(kr) \sin \eta_l] - k^3 r^2 \left( 1 - \frac{c_\infty^2}{c_0^2} \right) \\ \times [j_l(kr) \cos \eta_l - n_l(kr) \sin \eta_l]^2. \quad (17) \end{aligned}$$

Here  $j_l$  and  $n_l$  are the spherical Bessel and Neumann functions, respectively, and the primes denote derivatives with respect to the arguments. The function  $\eta_l(r)$  is to be interpreted as the phase shift which would result if one set  $\rho_0 = \rho_\infty$  and  $c_0 = c_\infty$  for radii greater than  $r$ ; i. e., if the scattering terms were cut off at  $r$ . The quantity one needs to calculate is of course the limiting value of  $\eta_l(r)$  at large  $r$ . The boundary condition at the core-structure radius becomes

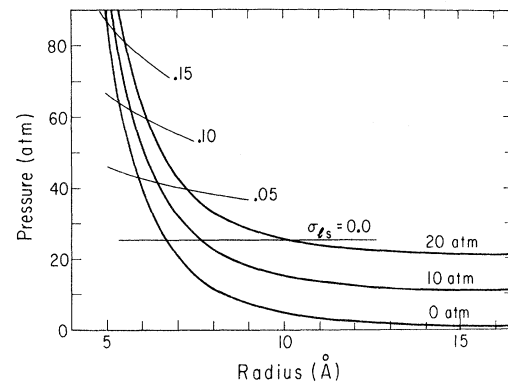


FIG. 2. Electrostrictive variation of fluid pressure with distance from an excess charge in liquid helium below 1.0 °K, for various values of the pressure at infinity. Also shown are curves determining the solidification radius, as discussed in the text.

$$\eta_l(a) = \arctan \left[ \frac{j_l'(ka) + \gamma_l ka j_l(ka)}{n_l'(ka) + \gamma_l ka n_l(ka)} \right], \quad (18)$$

where, following the notation of Baym *et al.*, we have written

$$\gamma_l = -\lambda_l \rho_0(a) c_\infty^2 / a. \quad (19)$$

The initial phase shifts given by Eq. (18) are those which arise from the central-core structure alone, and thus describe the scattering when the electrostrictive effects in the surrounding fluid are ignored.

### V. MISCELLANEOUS REMARKS

Equation (17) and (18) do not provide much direct insight into what is going on, but they are very well suited to quantitative numerical calculations. We are in any case forced to take a somewhat numerical approach in what follows for several reasons: The phonon wavelengths of primary interest are of order the size of the scatters so that many partial waves are necessary for convergence<sup>13</sup>;  $\rho_0(r)$  and  $c_0(r)$  which appear in Eq. (17) are numerically specified functions which must be obtained at each step of the integration by solving Eq. (7); and finally, we are interested in making quantitative numerical comparisons with experiment.

The experimental data particularly germane to our discussion are the recent measurements<sup>2-4</sup> of carrier mobilities below 1 °K. We recall that an electric field  $\mathcal{E}$  is applied to the charge carriers, which then attain a mean drift velocity  $v_D$  proportional to  $\mathcal{E}$ , if  $\mathcal{E}$  is kept small enough. Conventionally one writes  $v_D = \mu \mathcal{E}$ , where  $\mu$  is the mobility. It is easy to see that the average force exerted by the excitation gas on the charge is then  $ev_D/\mu$ , and that the amount of momentum exchanged per cm of travel is just  $e/\mu$ . It has been shown by Baym *et al.*<sup>7</sup> that

$$\frac{e}{\mu} = -\frac{\hbar}{6\pi^2} \int_0^\infty k^4 \frac{\partial n}{\partial k} \sigma_T(k) dk, \quad (20)$$

where  $n$  is the distribution function of the elementary excitations under consideration and  $\sigma_T(k)$  is the momentum-transfer cross section

$$\sigma_T(k) = \int (1 - \cos\theta) \sigma(k, \theta) d\Omega, \quad (21)$$

where, in our case,

$$\sigma(k, \theta) = k^{-2} \left| \sum_{l=0}^{\infty} (2l+1) P_l(\cos\theta) \sin\eta_l e^{i\eta_l} \right|^2. \quad (22)$$

Of the approximations which are made in deriving Eq. (20) the most important is the neglect of recoil effects, an approximation which is certainly valid for phonon scattering but which becomes questionable when applied to the roton-limited regime.

Our task in Secs. VI–VIII will be to pick a likely model for the central-core structure, calculate the

phase shifts from Eqs. (17)–(19), and then use Eqs. (20)–(22) to find  $e/\mu$  as a function of temperature. The validity of our model for phonon scattering can then be tested by comparing the calculated  $e/\mu$  with the experimental data. Before plunging into detail, some preliminary comments may prove of value. First, we plot in Fig. 3 the thermal weight factor  $k^4(\partial n/\partial k)$  for phonons at several temperatures and zero pressure. Although the number of thermally activated phonons increases with  $T$ , their importance relative to rotons rapidly becomes small above  $T \sim 0.5$  °K. Therefore we can conclude from Fig. 3 that typical wavelengths of interest are greater than about 15 Å. Since this is well within the linear region of the excitation spectrum, the use of Eq. (5) is justified. From Eq. (20) it is easy to see that if  $\sigma_T(k)$  goes as  $k^n$ , then  $e/\mu$  will exhibit a  $T^{n+4}$  dependence on temperature, the  $T^4$  term arising from the variation of the thermal-weight curve with temperature.

Another feature of general interest is the relative importance in the phonon-scattering process of the electrostrictive variations in the fluid surrounding the core structure of the charge carrier. One may ask if the integration of Eq. (17) will result in only a minor adjustment of the phase shifts, or whether it will in fact be the dominant effect. To answer this question, we show in Fig. 4 the first few  $\eta_l(r)$ 's, calculated at  $k = 0.1 \times 10^8$  for a rigid immovable central core ( $\gamma_l = 0$ ) of radius 5.5 Å. It is immediately clear that for the positive carrier the electrostrictive variations in the fluid outside the core are a major factor in determining the scattering. Our previous treatment<sup>3</sup> in which only the effect of the core in the long-wavelength limit was considered is therefore oversimplified. Turning to the negative carriers, one notes from Fig. 4 that  $\eta_l(r)$  changes only slightly beyond 15 Å.

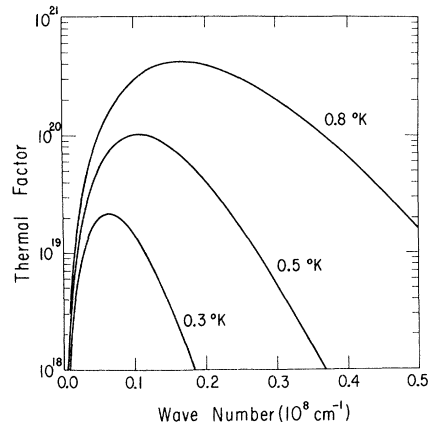


FIG. 3. Thermal weight factor  $k^4(\partial n/\partial k)$  for phonons in liquid helium at temperatures of interest.

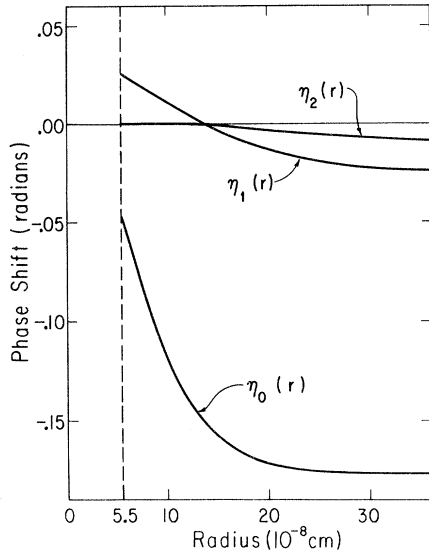


FIG. 4. Result of a typical numerical phase-shift integration, including the effects of electrostriction in the fluid surrounding the core. This example corresponds to a phonon of wave number  $0.1 \times 10^8 \text{ cm}^{-1}$  and an immovable, hard core of radius of  $5.5 \text{ \AA}$ .

Indeed, it has already been demonstrated by Baym *et al.*<sup>7</sup> that taking only the effect of the bubble into account is sufficient to give good agreement with experiment. In sum, Fig. 4 leads us to the qualitative expectation that for positive carriers  $\sigma_T(k)$  should depend strongly on scattering from the fluid surrounding the core. For negatives, on the other hand, the boundary conditions at the bubble surface will dominate  $\sigma_T(k)$ , with a small but perhaps significant correction arising from electrostrictive effects.

#### VI. PHONON SCATTERING BY POSITIVE CHARGE CARRIERS

We first consider the properties of the core surrounding the positive charge. Because of the very small distances involved, the description of the core given below is valid only in an average and approximate sense. On the other hand, a sound wave really does sample the average properties of the charge carrier, and one may expect that the scattering process will be sensitive only to the gross features of the core.

It was suggested by Atkins<sup>6</sup> in his original paper that as the charge is approached and the electrostrictive pressure in the liquid rises to the melting pressure  $p_m$ , a liquid-solid phase transition occurs, resulting in a solid core. More precisely, if one includes a possible liquid-solid surface energy density  $\sigma_{ls}$ , the transition will occur at an average radius  $a_*$  given by

$$p_0(a_*) = p_m + \frac{2\sigma_{ls}}{a_*} \frac{v_s}{v_l - v_s}, \quad (23)$$

where  $p_0$  is the pressure in the liquid, and  $v_l$  and  $v_s$  are the molar volumes of the liquid and the solid, respectively, at the melting pressure. The missing element in this prescription for determining  $a_*$  is  $\sigma_{ls}$ , which is not a well-known quantity. However, recent measurements<sup>14-16</sup> of  $e/\mu_*$  near the melting pressure have yielded strong evidence that  $\sigma_{ls}$  is nonzero and of order  $0.1 \text{ erg cm}^{-2}$ . The value of  $a_*$  corresponding to  $\sigma_{ls}$  can easily be determined graphically, as in Fig. 2, by finding the intersection of the  $p_0(r)$  and the  $p_m + (2\sigma_{ls}/r)v_s(v_l - v_s)^{-1}$  curves. The second row of Table I gives the values of  $a_*$  corresponding to various  $\sigma_{ls}$  in the range of interest.

In addition to the radius of the core, one also needs to determine the response coefficients  $\lambda_l$  defined by Eq. (15). The response of the core to the sound-pressure field can be expected to be somewhat peculiar, since a local increase in pressure causes the phase boundary to move outward. If a small excess pressure  $\delta p(\theta)$  is added to  $p_0(a_*)$ , the new boundary of the core  $a(\theta)$  will be given by

$$p[a(\theta)] + \delta p(\theta) = p_m + \frac{2\sigma_{ls}}{a(\theta)} \frac{v_s}{v_l - v_s}. \quad (24)$$

Expanding  $\delta p(\theta)$  and  $a(\theta)$  in spherical harmonics as before then immediately yields

$$\lambda_l = - \left( \left. \frac{\partial p_0}{\partial r} \right|_{r=a_*} + \frac{2\sigma_{ls}}{a_*} \frac{v_s}{v_l - v_s} \right)^{-1}, \quad l=0, 2, 3, \dots \quad (25)$$

The  $\partial p_0/\partial r$  term in Eq. (25) is easily evaluated, e. g., from Fig. 2, and the resulting values of  $\lambda_l$  are given in the fifth row of Table I.

Note that the  $l=1$  coefficient is explicitly omitted from Eq. (25). The  $l=1$  partial-pressure wave exerts a net force on the core, and the resulting motion must be taken into account by adding a term  $\Delta\lambda_1$  of the well-known form<sup>10</sup>

$$\Delta\lambda_1 = \frac{4}{3} \pi \frac{a_*^4}{c_s^2 M_*} \frac{1}{(ka_*)^2} \quad (26)$$

to the expression in Eq. (25).  $M_*$  is the mass of the core, a quantity which may be calculated ap-

TABLE I. Positive core parameters for various values of  $\sigma_{ls}$ . The meanings of the various parameters are discussed in the text.

| $\sigma_{ls}$              | erg cm <sup>-2</sup>                                   | 0.00  | 0.05  | 0.10  | 0.15  |
|----------------------------|--|-------|-------|-------|-------|
| $a_*$                      | ( $\text{\AA}$ )                                       | 6.66  | 5.89  | 5.37  | 5.00  |
| $\rho_0(a_*)$              | (g cm <sup>-3</sup> )                                  | 0.172 | 0.184 | 0.194 | 0.204 |
| $M_*$                      | (He <sup>4</sup> masses)                               | 47    | 35    | 29    | 24    |
| $\lambda_{l \neq 1}$       | (10 <sup>-16</sup> dyn <sup>-1</sup> cm <sup>3</sup> ) | 6.29  | 3.46  | 2.24  | 1.59  |
| $\Delta\lambda_1 (ka_*)^2$ | (10 <sup>-16</sup> dyn <sup>-1</sup> cm <sup>3</sup> ) | 4.68  | 3.86  | 3.23  | 2.88  |

proximately from the electrostriction model as follows. The equation of state of solid helium<sup>17,18</sup> may be written to sufficient accuracy as

$$p_s = p_m + D_1(\rho - \rho_{s0}) + D_2(\rho - \rho_{s0})^2 + D_3(\rho - \rho_{s0})^3, \quad (27)$$

where  $\rho_{s0} = 0.190$ ,  $p_m = 2.53 \times 10^7$ ,  $D_1 = 1.33 \times 10^9$ ,  $D_2 = 1.52 \times 10^{10}$ ,  $D_3 = 1.96 \times 10^{11}$ , all in cgs units. The equation determining the density as a function of radius inside the core then has the same form as Eq. (7) with, of course, different constants. The initial density  $\rho$  at  $r = a_*$  is given by the requirement that in the solid at  $r = a_*$  the pressure must be  $p_0(a_*) + 2\sigma_{1s}/a_*$ , and  $\rho_2(r)$  is then found the same way as before. Although  $\rho_2(r)$  calculated in this way diverges as  $r \rightarrow 0$ , it does so more slowly than  $r^{-2}$  and  $M_*$  is well defined. The results of our calculations of  $M_*$  are given in the fourth row of Table I, in terms of He<sup>4</sup> masses. The corresponding values of  $\Delta\lambda_1$  are given in the sixth row. Since  $ka_*$  in the region of interest is of order 1 or less,  $\Delta\lambda_1$  is an important contribution to  $\lambda_1$ .

Once the proper characterization of the core has been established, one can apply the formalism of Secs. IV and V. On the basis of previous experiments<sup>16</sup> we choose the core properties corresponding to  $\sigma_{1s} = 0.10$  as the best initial guess. The importance of the various refinements that have been introduced here is illustrated in Fig. 5. Curve 1 is the calculated momentum-transfer cross section for an immovable hard sphere ( $\lambda_l = 0$ ) of radius  $a = 5.37 \text{ \AA}$ , without including any of the effects of electrostriction in the fluid surrounding the core.

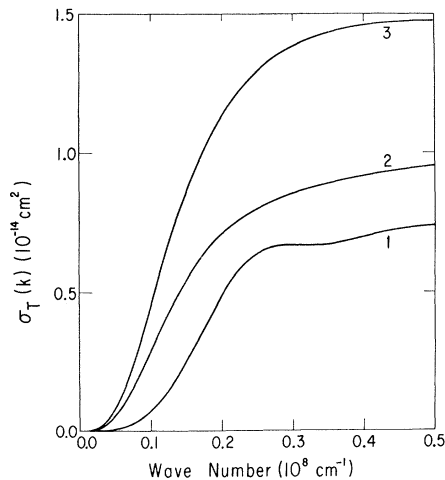


FIG. 5. Momentum-transfer cross section  $\sigma_T(k)$  for phonons scattered by a core structure of radius  $5.37 \text{ \AA}$ . Curve 1: immovable hard core with electrostrictive effects in the surrounding fluid neglected; curve 2: immovable hard core with electrostriction included; curve 3: immovable responsive core with electrostriction included.

Curve 2 was calculated using the same boundary conditions, but here the electrostrictive effects were explicitly included by means of the formalism of Sec. IV. As indicated by our earlier qualitative discussion, the scattering is greatly altered, particularly in the region below  $k = 0.2 \times 10^8 \text{ cm}^{-1}$ , where our main interest is concentrated. The results of the complete calculation including electrostriction and the response parameters of Eqs. (25) and (26) are given by curve 3. It is clear that the "refinements" we have introduced in fact dominate  $\sigma_T(k)$ , leading to a prediction  $e/\mu$  which is about a factor of 5 larger than the hard-sphere value.

Once results such as curve 3 in Fig. 5 have been obtained, it is a simple matter to calculate  $e/\mu_*$  as a function of  $T$  from Eq. (20). Figure 6 shows the experimental values of  $e/\mu_*(T)$ , along with the theoretical values predicted for the various  $\sigma_{1s}$ 's of Table I. The agreement between experiment and our calculations is seen to be very good indeed, in that  $\sigma_{1s} = 0.1 \text{ erg cm}^{-2}$ , which was a rough value derived from a quite different experiment, leads to a predicted  $e/\mu_*(T)$  within 10% of the measured values. A completely satisfactory fit is obtained with  $\sigma_{1s} = (0.135 \pm 0.010) \text{ erg cm}^{-2}$  corresponding to a core radius of  $(5.1 \pm 0.1) \text{ \AA}$ ; but in view of the approximations made in deriving Eq. (11) this improvement is probably not too meaningful.

#### VII. PHONON SCATTERING BY NEGATIVE CHARGE CARRIERS

The accepted picture of the central structure of the negative carrier is that of an electron localized in a bubble from which the He<sup>4</sup> atoms are excluded. The radius  $a_-$  of the bubble is determined by minimizing the total energy,<sup>19</sup>

$$E = E_{e1} + 4\pi\sigma r^2 + \frac{4}{3}\pi p r^3 - \frac{1}{2} \frac{(\kappa - 1)}{\kappa} \frac{e^2}{r}, \quad (28)$$

where  $E_{e1}$  is the energy of the electron localized in the cavity,  $\sigma$  is the surface energy density,  $p$  is the pressure in the liquid, and  $\kappa$  is the dielectric constant. The last term arises from electrostriction and represents only a very small correction. An important assumption implicit in Eq. (28) is that the surface of the bubble is sharply defined. Actually, the average liquid-helium density must vary smoothly with radius, going from zero to the bulk value. The range in  $r$  over which this happens has been estimated<sup>20</sup> to be of order  $1-2 \text{ \AA}$ , i. e.,  $\approx 10\%$  of the radius of the bubble. One therefore expects that calculations of the scattering cross section which are based on the idealized bubble model and thus ignore the effects of the surface transition region will be good to about 20%. To first order  $E_{e1}$  may be evaluated by assuming that the liquid outside the bubble is dense enough so that the wave function of the electron is zero at

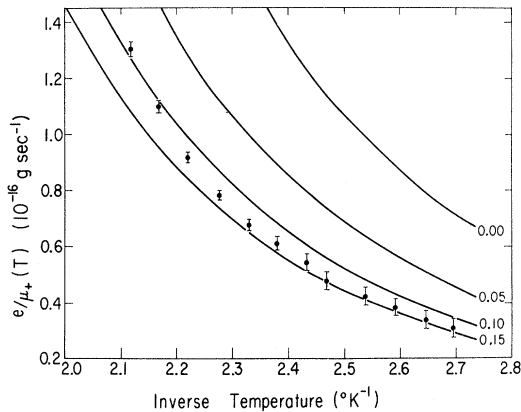


FIG. 6. Points are the experimental values of  $e/\mu_+$  in the phonon-dominated temperature region, while the curves give the theoretically predicted behavior using the core parameters corresponding to various assumed values of  $\sigma_{1s}$ . The deviation for  $T^{-1} < 2.25$  is due to rotons.

$\gamma = a_-$ . In reality  $\Psi_{e1}$  extends somewhat into the fluid, and the more accurate evaluations of  $E_{e1}$  are an excessively complicated problem: Both the boundary conditions on the electron wave function presented by the individual  $\text{He}^4$  atoms and the unknown variation of the fluid density in the surface transition region must be taken into account. A rough estimate of the correction to  $E_{e1}$  due to the first of these effects has been given by Springett, Cohen, and Jortner,<sup>19</sup> who find that in liquid helium the penetration of the electron wave function results in a decrease in  $a_-$  of about 5%.

A somewhat different approach is to characterize the decay of the electron wave function in the liquid by a parameter  $V_1$ , such that  $\Psi_{e1} \propto r^{-1} e^{-Kr}$ , where  $K = \hbar^{-1} [2m(V_1 - E_{e1})]^{1/2}$ . All of the detailed complications of what happens near the surface of the bubble are then roughly lumped into one unknown number. Defined in this way,  $V_1$  plays the role of an effective well depth for the electron, but the reader should note that  $V_1$  is not necessarily the energy required to inject any electron into a delocalized state: The properties of the liquid very near the surface of the bubble are probably quite anomalous. If  $V_1$  is given, Eq. (28) yields  $a_-$  provided  $\sigma$  is known. Since there are some difficulties associated with the correct value of  $\sigma$  to use in Eq. (28), we will consider  $a_-$  and  $V_1$  as variable parameters with which to fit the data.

Celli *et al.*<sup>11</sup> have given a complete and elegant discussion of sound scattering from an idealized electron bubble characterized as described above by the parameters  $a_-$  and  $V_1$ . Their results were applied successfully by Baym *et al.*<sup>7</sup> to explain the observed  $e/\mu_-(T)$  in the phonon-limited regime. The results described in the remainder of this sec-

tion are a simple extension of the work of these authors.

We calculated  $e/\mu_-(T)$  for a wide range of values of  $a_-$  and  $V_1$ , in order to see how sensitive the agreement between theory and experiment is to variations in these parameters. The  $\gamma_i$ 's of Eqs. (18) and (19) were determined according to the method of Celli *et al.*,<sup>11</sup> and electrostrictive effects were initially neglected so that the resulting phase shifts  $\eta_i(a)$  directly determined  $\sigma_T(k)$ . A typical calculated  $\sigma_T(k)$  curve is shown in Fig. 7, which nicely exhibits the various resonances in the momentum-transfer cross section that arise from the resonant modes of vibration of the bubble. The fractional deviations between the experimental and the calculated  $e/\mu_-$  are shown in Figs. 8(a) and 8(b) for various values of  $a_-$  and  $V_1$ . These curves show a complicated dependence on the parameters, but they do lead to several interesting conclusions. As was pointed out earlier by Baym *et al.*, the general fit is quite good. However, it is noteworthy that the measured  $e/\mu_-$  is 20–30% higher than the theoretical, for all values of  $a_-$ ,  $V_1$  in the range of interest. This probably arises from our use of a somewhat idealized scattering model, no account having been taken of the effect of the transition region at the bubble surface on the sound scattering. Detailed calculations by the method used for positive ions show that the effect of electrostriction on  $e/\mu_-$  produces changes of less than 1 or 2%, and hence this mechanism cannot account for the excess scattering that is observed.

One may also note that  $e/\mu_-$  varies only very weakly with the parameters  $a_-$  and  $V_1$ . The shape of the  $\sigma_T(k)$  curve depends rather strongly on these parameters. However, one finds that the manner in which  $\sigma_T(k)$  tails off on the large- $k$  side of the

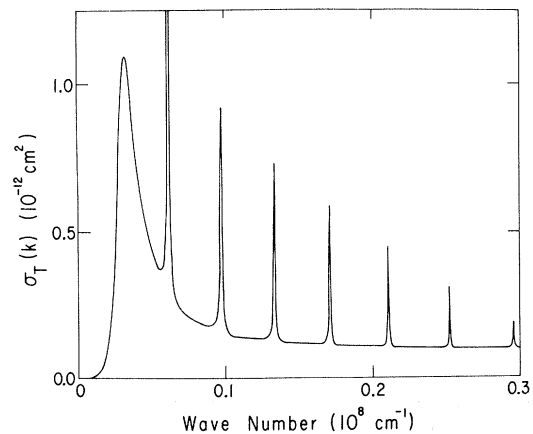


FIG. 7. Momentum-transfer cross section  $\sigma_T(k)$  for phonons scattered by an electron bubble. The bubble parameters in this example are  $a_- = 16 \text{ \AA}$ ,  $V_1 = 0.6 \text{ eV}$ .

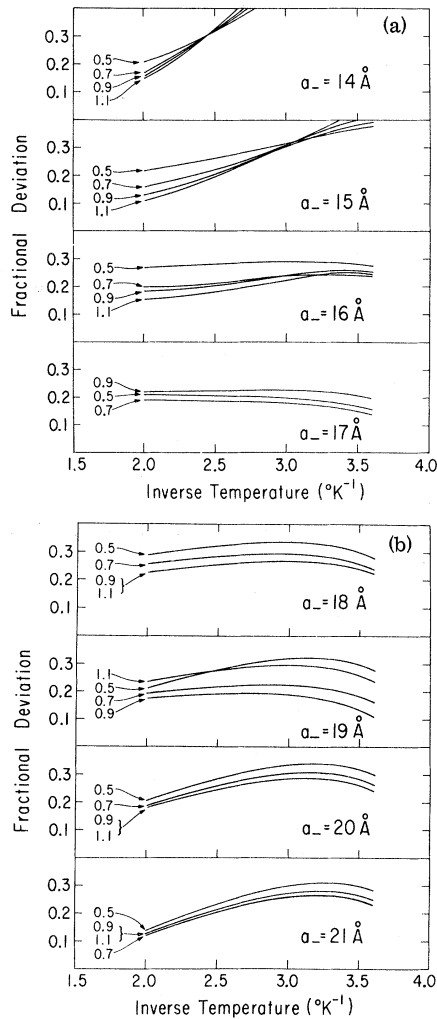


FIG. 8. Fractional deviation  $[(e/\mu_-)_{\text{expt}} - (e/\mu_-)_{\text{th}}]/(e/\mu_-)_{\text{th}}$  as a function of inverse temperature for various values of the bubble parameters  $a_-$  and  $V_1$ .

dominant  $s$ -wave resonance depends only weakly on  $\gamma_0$ . It is in this tailing-off region that the thermal factor is concentrated, and, since the higher-order partial waves are much less important, one cannot affect  $e/\mu_-$  very much by varying the  $\gamma_i$ 's; hence the weak dependence on the bubble parameters. As an unhappy consequence, not very much can be learned about the electron bubble from  $e/\mu_-$  in the phonon-limited region. One can conclude that the best over-all fit between theory and experiment is found for  $a_-$  in the range 16–19 Å, with the additional observation that the fit rapidly becomes very poor for  $a_-$  below 16 Å. No definite conclusions about  $V_1$  can be drawn.

### VIII. ROTON SCATTERING

Once an adequate theory of phonon scattering has been established, the roton contribution to  $e/\mu$

can be determined by subtracting from the measured values the putative phonon contribution in the temperature region where the two overlap significantly. For positives, the phonon contribution (see Fig. 6) was calculated using the best-fit values of the core parameters corresponding to  $\sigma_{ts} = 0.135$  erg cm $^{-2}$ . For negatives we took  $e/\mu_-(T)$  calculated for  $a_- = 17$  Å,  $V_1 = 0.7$  eV and multiplied it by a correction factor which brings theory and experiment into agreement at  $T = 0.5$  °K. To determine the likely error introduced by this heuristic procedure, the same process was carried out for several sets of parameters  $a_-$ ,  $V_1$  within the reasonable range. The resulting empirically corrected phonon curves differed by less than 2% in the range  $1.0 \geq T \geq 0.5$  °K, and we take this as a reasonable error estimate. From a fundamental point of view such a procedure is not very satisfactory, but it is perhaps the best to be done at present.

The contributions to  $e/\mu(T)$  from roton scattering are shown in Fig. 9. The dominant exponential temperature dependence arising from the roton energy gap $^{21}$   $\Delta/k = (8.65 \pm 0.04)$  °K has been divided out for convenience of representation. These data exhibit two interesting qualitative features of roton scattering. First, from the data for the positives one sees that a considerable variation with temperature remains when the exponential factor has been eliminated. In fact, the simple expression

$$e/\mu_+ = 1.34 \times 10^9 T^{-1/2} e^{-\Delta/kT} \quad (29)$$

gives a quite satisfactory fit to the data. Data for the negatives are not good enough to provide such detailed information on the temperature dependence of the prefactor to the exponential, but it seems to fall between  $T^0$  and  $T^{-1/2}$ . The approximate  $T^{-1/2}$  dependence of the prefactor observed for positives

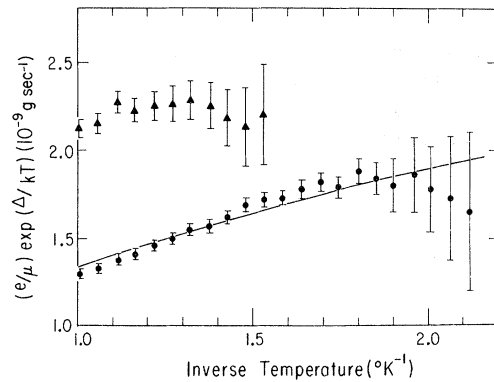


FIG. 9. Roton contribution to  $e/\mu$  for positive (circles) and negative (triangles) carriers. The exponential temperature dependence has been divided out. The curve through the positive carrier data has the equation  $(e/\mu_+) \times e^{8.65/T} = 1.34 \times 10^9 T^{-1/2}$ .

(and perhaps for negatives) is surprising. The roton number density goes as  $T^{1/2} e^{-\Delta/kT}$ , and the simplest kinetic-theory arguments<sup>1</sup> give a  $T^1$  dependence of the prefactor. A more serious treatment<sup>3,7</sup> which takes account of the very large effective masses of the charge carriers, yields a temperature-independent prefactor, though even here severe approximations have been made, including the neglect of recoil effects and the neglect of the variation of  $\sigma_T(k)$  near the roton minimum.

The second interesting feature of Fig. 9 is the relatively small difference between  $e/\mu$  for negative and positive carriers.<sup>22</sup> With core-structure radii of  $\sim 17 \text{ \AA}$  for negatives and  $\sim 5 \text{ \AA}$  for positives, one might naively expect that  $e/\mu_-$  be a factor of 10 larger than  $e/\mu_+$ . In fact, the observed ratio is about 1.5. One possible explanation is that, as in phonon scattering, the electrostrictive density variation in the fluid surrounding the positive core contributes heavily to the roton scattering. Other factors which may be important are the disparate boundary conditions presented by the two core

structures, and the difference in the effective masses of the two carriers.

It seems that the data shown in Fig. 9 require a substantial modification of the simple theory based on the formalism of Baym *et al.* Some interesting attempts to calculate  $\sigma_T(k)$  for roton scattering have appeared recently,<sup>23,24</sup> but not in a form easily tested against experiment. More work on this problem is clearly required.

*Note added in proof.* As discussed in Sec. VII, no set of  $\gamma_i$ 's derived from the bubble model with reasonable values for  $a_-$  and  $V_1$  gives complete agreement with the experimentally observed behavior of the negative carriers. It has, however, been pointed out to us by R. G. Barrera and G. Baym that if the  $\gamma_i$ 's themselves are treated as free parameters, a perfect fit to experiment can easily be obtained.

#### ACKNOWLEDGMENT

This research has been supported in part by the Advanced Research Projects Agency.

<sup>1</sup>F. Reif and L. Meyer, Phys. Rev. **119**, 1164 (1960).

<sup>2</sup>K. W. Schwarz and R. W. Stark, Phys. Rev. Letters **21**, 967 (1968).

<sup>3</sup>K. W. Schwarz and R. W. Stark, Phys. Rev. Letters **22**, 1278 (1969).

<sup>4</sup>K. W. Schwarz, Phys. Rev. A (to be published).

<sup>5</sup>C. G. Kuper, Phys. Rev. **122**, 1007 (1961).

<sup>6</sup>K. R. Atkins, Phys. Rev. **116**, 1339 (1959).

<sup>7</sup>G. Baym, R. G. Barrera, and C. J. Pethick, Phys. Rev. Letters **22**, 20 (1969).

<sup>8</sup>B. M. Abraham, Y. Eckstein, J. B. Ketterson, M. Kuchnir, and P. R. Roach, Phys. Rev. A **1**, 250 (1970).

<sup>9</sup>A. J. Dahm and T. M. Sanders, Jr., Phys. Rev. Letters **17**, 126 (1966).

<sup>10</sup>H. Lamb, *Hydrodynamics* (Dover, New York, 1945), Chap. 10.

<sup>11</sup>V. Celli, M. H. Cohen, and M. J. Zuckerman, Phys. Rev. **173**, 253 (1968).

<sup>12</sup>B. R. Levy and J. B. Keller, J. Math. Phys. **4**, 54 (1963).

<sup>13</sup>30 partial waves were used in all calculations.

<sup>14</sup>K. O. Keshishev, Yu. Z. Kovdrya, L. P. Mezhov-Deglin, and A. I. Shal'nikov, Zh. Eksperim. i Teor. Fiz. **56**, 94 (1969) [Sov. Phys. JETP **29**, 53 (1969)].

<sup>15</sup>B. A. Brody, thesis (University of Michigan, 1970) (unpublished).

<sup>16</sup>R. M. Ostermeier and K. W. Schwarz, Phys. Rev. (to be published).

<sup>17</sup>See references in J. Wilks, *Liquid and Solid Helium* (Clarendon, Oxford, 1967), Chap. 21.

<sup>18</sup>J. W. Stewart, Phys. Rev. **129**, 1950 (1963).

<sup>19</sup>B. F. Springett, M. H. Cohen, and J. Jortner, Phys. Rev. **159**, 183 (1967).

<sup>20</sup>K. Hiroike, N. R. Kestner, S. A. Rice, and J. Jortner, J. Chem. Phys. **43**, 2625 (1965).

<sup>21</sup>D. G. Henshaw and A. D. B. Woods, Phys. Rev. **121**, 1266 (1961).

<sup>22</sup>This has also been pointed out by B. A. Brody (Ref. 15) on the basis of measurements made above 1°K.

<sup>23</sup>I. Iguchi, J. Low Temp. Phys. **4**, 637 (1971).

<sup>24</sup>G. G. Ihas, thesis (University of Michigan, 1971) (unpublished).